http://dx.doi.org/10.62762/TSCC.2025.731885

RESEARCH ARTICLE

Computational Experimental Test on PID Controlled Fixed Wing Aircraft Systems

Eileen Horstkötter[1] **and Quanmin Zhu**[1,*]

[1] School of Engineering, University of the West of England, Bristol BS16 1QY, United Kingdom

Abstract

This paper focuses on the implementation of a control framework for a fixed wing aircraft system and the simulation demonstrations. The aim is to develop several Proportional Integral Derivative (PID) controllers to stabilise the altitude and attitude in a 2D environment by regulating the engine power, the pitch angle, and height in flight operation. In technique, a dynamic mathematical model is established by considering the degrees of freedom and the dynamics of motion of a fixed wing aircraft, which provide a foundation for design and simulation. A simplified aircraft dynamic model is tailored for testing the formed control systems, which can be flexibly modified with different aircraft configurations, for a showcase illustration a calculation of the moment of inertia is included. Further, several flight settings such as height differences and velocities are proposed and a feasible implementation of the PID controllers is introduced for adjusting the control variables, and further a switching mode with two controllers for the height with different speeds are simulated to select the height linked controllers.

Keywords: aircraft dynamic modelling, control systems, PID, simulation, Matlab/Simulink.

Nomenclature

Symbol	Description	Unit
F_e	Force of the engine	N
F_D	Drag force	N
p	pressure	Pa
m	mass	kg
$\ddot{X}$	Acceleration in x direction	$\frac{m}{s^2}$
$\dot{X}$	Velocity x direction	$\frac{m}{s}$
X	Distance in x direction	m
F_{eng}	Force engine	N
F_{Dw}	Drag force wing	N
F_{Dfl}	Drag force flaps	N
F_{Del}	Drag force elevator	N
F_{Dfll}	Drag force flaps left	N
F_{Dflr}	Drag force flaps right	N
F_L	Lift force	N
g	Acceleration of gravity	$\frac{m}{s^2}$
$\ddot{Z}$	Acceleration in z direction	$\frac{m}{s^2}$
$\dot{Z}$	Velocity in z direction	$\frac{m}{s}$
Z	distance in z direction	m
F_{Lw}	Lift force wing	N
F_{Lfl}	Lift force flaps	N

Submitted: 14 February 2025
Accepted: 11 May 2025
Published: 18 May 2025

Vol. 2, **No.** 2, 2025.
10.62762/TSCC.2025.731885

***Corresponding author:**
✉ Quanmin Zhu
quan.zhu@uwe.ac.uk

Citation
Horstkötter, E., & Zhu, Q. (2025). Computational Experimental Test on PID Controlled Fixed Wing Aircraft Systems. *ICCK Transactions on Sensing, Communication, and Control*, 2(2), 95–105.

Symbol	Description	Unit
F_{Lel}	Lift force elevator	N
F_{Lfll}	Lift force flaps left	N
F_{Lflr}	Lift force flaps right	N
J	Mass moment of inertia	kgm^2
$\ddot{\theta}$	Acceleration pitch	$\frac{m}{s^2}$
$M_{inherit}$	Moment of inertia	Nm
$\dot{\theta}$	Velocity pitch	$\frac{m}{s}$
θ	Pitch angle	$^\circ$
ρ	density	$\frac{kg}{m^3}$
ρ	velocity	$\frac{m}{s}$
c_l	Lift coefficient	-
A	Wing area	m^2
F_{Df}	Frictional drag	N
F_{Dp}	Pressure drag	N
c_{Df}	Friction drag coefficient	-
c_{Dp}	Pressure drag coefficient	-
A_{st}	Area subject to flow	m^2
c_p	Centre of pressure	-
AoA	Angle of attack	$^\circ$
F_G	Gravity force	N
x_w	x-axis world frame	-
x_B	x-axis body frame	-
x_l	X-axis air frame	-
u	Controller input	-
K_p	Proportional vale	-
K_i	Integral value	-
K_d	Derivative value	-
f_b	Fuel burn	m^3
k	Spring constant	$\frac{N}{m}$

1 Introduction

Fixed-wing aircraft are flying vehicles with non-rotating wings that generate lift due to forward motion through the air [1], which have been widely used across civil, military, research, and commercial sectors. There is a long list of examples and real-world applications, regarding the aircraft: 1) Manmade aircraft with commercial airlines from Boeing and Airbus, various private and general aviation with Cessna, Piper, and Diamond, 2) Unmanned Aerial Vehicles (UAVs) / Drones with small UAVs for surveying, tactical military drones, high-altitude long endurance (HALE) UAVs. Regarding the applications, it has expanded to include passenger transport, cargo and freight, aerial surveying and mapping, precision agriculture, aerial monitoring, and life-saving deliveries, among others [2].

High safety standards are essential in the operation of such aircraft, given the critical nature of aviation and the potential consequences of system failures. These safety standards are not only enforced through strict regulatory frameworks and maintenance protocols but also achieved through the implementation of advanced control systems. One of the key strategies in modern aircraft design is the use of closed-loop control systems, which continuously monitor the aircraft's state and automatically adjust various parameters to ensure stable and safe operation. These systems play a crucial role in assisting the pilot by managing tasks such as maintaining altitude, speed, and heading, as well as handling complex functions like autopilot, fly-by-wire control, and engine management. By doing so, they significantly reduce the pilot's workload, minimise the likelihood of human error, and contribute to the overall safety and efficiency of flight operations. The integration of automation and feedback mechanisms ensures that the aircraft can respond rapidly and accurately to changing conditions, thereby enhancing both performance and safety margins.

A wide range of control methods has been developed and applied to fixed-wing aircraft systems, encompassing both classical and modern control approaches. Classical methods such as proportional-integral-derivative (PID) control [3], linear-quadratic regulators (LQR) [4], and H-infinity control [5] have been widely used in both academic research and industrial applications. More recently, advanced techniques like model predictive control (MPC) [6], adaptive control [7], robust control [8], and artificial intelligence-based methods [9] have gained attention due to their ability to handle nonlinearities, uncertainties, and complex mission requirements.

Despite these advancements, PID control remains the most adopted approach in practical fixed-wing aircraft control systems. This continued prevalence is largely due to the simplicity, reliability, and intuitive nature of PID controllers [3]. They are straightforward to implement, require minimal computational resources, and offer sufficient performance for a wide range of flight conditions and mission profiles. Moreover, one of the most compelling advantages of PID control is the ease with which controller gains can be tuned and adjusted. This aspect is particularly important in operational settings where human operators — such as engineers, test pilots, or maintenance personnel — may need to directly interact with the control system for fine-tuning or adaptation. The transparency and predictability of PID control facilitate this interaction, making it easier to diagnose issues, adjust system behaviour, and ensure safety. In summary, while advanced control methods offer theoretical performance improvements and flexibility, PID control remains the cornerstone of fixed-wing aircraft control

systems due to its practicality, robustness, and user-friendly nature — especially in environments where operator involvement in controller tuning is critical.

Understanding the dynamic models of fixed-wing aircraft is crucial for designing, analyzing, and implementing effective flight control systems [10]. These models describe how an aircraft responds to control inputs, external disturbances, and aerodynamic forces over time. By capturing the complex interactions between the aircraft's structure, propulsion, and environmental influences, such as wind and turbulence, dynamic models enable engineers and researchers to predict the aircraft's behavior under various flight conditions. Proper dynamic modelling is essential for achieving stability and controllability—two fundamental requirements in aviation [11]. With a well-defined model, control algorithms can be designed to ensure that the aircraft maintains desired trajectories, handles disturbances gracefully, and responds predictably to pilot or autopilot commands. This is especially important in autonomous systems, where the aircraft must make real-time decisions based on its understanding of its own dynamics and the environment. Moreover, dynamic models serve as the foundation for simulation, training, fault detection, and performance optimisation [12]. In simulation environments, they enable safe and cost-effective testing of new control strategies and flight maneuvers without risking physical hardware. For manned and unmanned aerial vehicles alike, a strong grasp of their dynamic behaviour is essential for ensuring flight safety, improving fuel efficiency, and achieving mission success in both civilian and military applications. In short, the dynamic modeling of fixed-wing aircraft is not just a theoretical exercise; it is a practical necessity that supports the entire lifecycle of aircraft development — from design, simulation, and testing to operation and maintenance.

The associated major contributions include the following:

1. Proposing a computational experimental framework for testing PID control schemes on fixed-wing aircraft using Matlab/Simulink.
2. Evaluating PID performance under various flight phases, offering detailed stability and robustness analysis.
3. Introducing a performance-based tuning methodology for PID gains tailored to fixed-wing flight dynamics.
4. Providing benchmarking results and releasing the simulation platform/codebase for facilitating future research and development.

The rest of the study include Section 2 modelling of an aircraft motion dynamics as the problem background, Section 3 designing the associated PID controllers as the solution for achieving the specified control system performance, Section 4 taking the computational experiments to test the design the control systems on the Simulink platform, and finally Section 5 summarising the study.

2 Dynamic modelling

2.1 Physics of an aircraft in 2D environment

An aircraft in the 2D environment has three degrees of freedom (DOF). An aircraft in a 2D environment has three degrees of freedom (DOF), which are movement along the longitudinal axis, movement along the vertical axis, and the pitch moment about the lateral axis. Therefore, it is essential to focus on the forces of the profile of an aircraft as shown in Figure 1 [13].

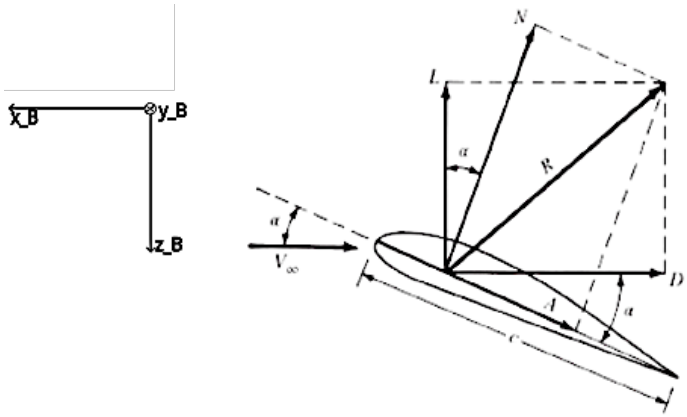

Figure 1. Forces on an aircraft profile.

The lift and drag forces are crucial. The Lift force is calculated as follows:

$$F_L = \frac{\rho}{2} * v^2 * c_l * A \tag{1}$$

The drag force is calculated theoretically from:

$$F_D = \int p_0 * dA * sin\varphi + \int r_0 * dA * cos\varphi \tag{2}$$

In realistic circumstances for an aircraft profile, it can be assumed as:

$$F_D = F_{Df} + F_{Dp} \tag{3}$$

whereas the frictional drag, F_{Df} is assumed as:

$$F_{Df} = \frac{\rho}{2} * v^2 * c_{Df} * A \tag{4}$$

The pressure drag F_{Dp} is derived from [14]:

$$F_{Dp} = \frac{\rho}{2} * v^2 * c_{Dp} * A_{st} \tag{5}$$

Therefore, the drag can be determined as:

$$F_D = \left(c_{Df} + c_{Dp} * \frac{A_{st}}{A}\right) * \frac{\rho}{2} * v^2 * A = c_D * \frac{\rho}{2} * v^2 * A \tag{6}$$

The lift and drag coefficient are calculated from the tested result of the NACA 0012 profile [15].

As shown in Figure 1 the forces of an air foil profile attack at the centre of pressure which depends on the angle of attack and can be calculated from [16]:

$$c_p = \frac{\int x * p(x)dx}{\int p(x)dx} \tag{7}$$

As stated in Figure 1, the resulting force of lift and drag is shown, which includes the lift and drag force. When thinking of an entire aircraft, the forces in the body frame can be derived from:

$$\overrightarrow{F_r} = \overrightarrow{F_{eng}} + \overrightarrow{F_g} + \overrightarrow{F_{rw}} + \overrightarrow{F_{r\,el}} \tag{8}$$

The total velocity of the aircraft in the flying direction can be calculated from:

$$v = \sqrt{(\dot{X}_w)^2 + (\dot{Z}_w)^2} \tag{9}$$

2.2 Kinematics of an aircraft - Forces in x-direction

The translational movement in the longitudinal direction is reached by the power of the engine of the aircraft. It includes several forces in the body frame as shown in Figure 2.

To derive the motion equation, the forces in x direction must be considered.

$$\sum Fix = 0 = F_{eng} - F_D - m{*}\ddot{X} \tag{10}$$

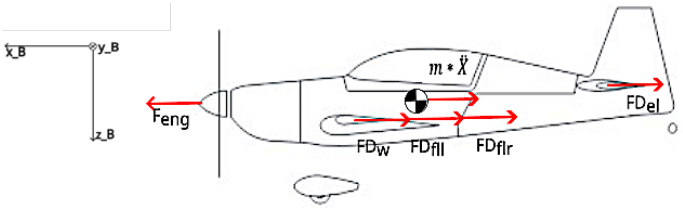

Figure 2. Forces x-axis Adapted from [17].

whereas m*$\ddot{X}$ is the inertia of the movement and the drag can be assumed as:

$$F_{Dfl} = FD_{fl_l} + FD_{fl_r} \tag{11}$$

$$F_D = F_{Dw} - F_{Dfl} - F_{Del} \tag{12}$$

With this the acceleration in the x – direction $(\ddot{X})$ can be determined by:

$$\ddot{X} = \frac{F_{eng} - F_{Dw} - F_{Dfl} - F_{Del}}{m} \tag{13}$$

Further, the velocity in x direction $(\dot{X})$ and the distance X can be derived from the integration:

$$X = \iint \frac{F_{eng} - F_{Dw} - F_{Dfl} - F_{Del}}{m}\, dtdt \tag{14}$$

2.3 Forces in z-direction

The vertical movement that generates a gain in altitude cannot be directly reached; therefore, it is achieved indirectly. With an increase in altitude, the aircraft also moves in the x-direction.

The equation of motion can be derived with:

$$\sum Fiz = 0 = -F_L + m * g + m * \ddot{Z} \tag{15}$$

The Lift F_L can be assumed as:

$$F_{Lfl} = FL_{fl_l} + FL_{fl_r} \tag{16}$$

$$F_L = F_{Lw} + F_{Lfl} + F_{Lel} \tag{17}$$

Equal to the longitudinal movement the acceleration $(\ddot{Z})$, the velocity $(\dot{Z})$ and distance (Z) can be derived:

$$Z = \iint \frac{F_{Lw} + F_{Lfl} + F_{Lel} - m * g}{m} dtdt \tag{18}$$

Like the equations in the x – direction integrations must be used.

2.4 Moment in 2D

The pitch angle theta is crucial to achieve the indirect movement in z – direction, in the body frame Figure 3.

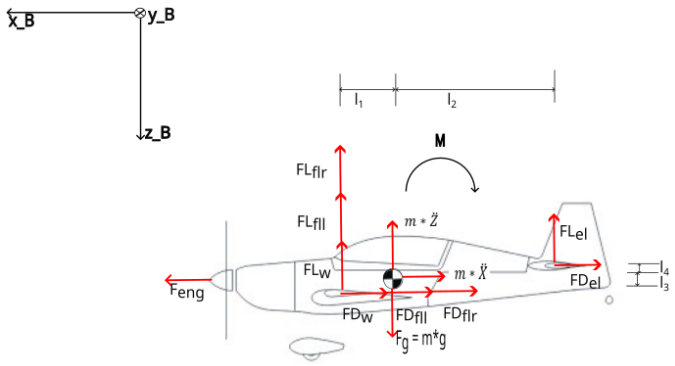

Figure 3. Moment along y-axis Adapted from [17].

The moment equation is derived from:

$$F_{Lfl} = FL_{fl_l} + FL_{fl_r} \tag{19}$$

$$F_{Dfl} = FD_{fl_l} + FD_{fl_r} \tag{20}$$

$$\sum Miy = 0 = -(F_{Lfl} + F_{Lw}) * l_1 - F_{Lel} * l_2 - (F_{Dfl} + F_{Dw} + F_{Del}) * l_3 + M \tag{21}$$

Whereas the moment is derived from:

$$M = J * \ddot{\theta} = M_{inherit} \tag{22}$$

The equation of movement for the moment is created by using the centre of gravity of the aircraft as the middle-fixed point as visualised in Figure 3.

The pitch acceleration $\ddot{\theta}$ can be derived equal to the vertical movement:

$$\ddot{\theta} = \frac{(F_{Lfl} + F_{Lw}) * l_1 + F_{Lel} * l_2}{J} + \frac{(F_{Dfl} + F_{Dw} + F_{Del}) * l_3}{J} \tag{23}$$

The pitch velocity $(\dot{\theta})$ and pitch angle (θ) is derived similar as before:

$$\theta = \iint \frac{(F_{Lfl} + F_{Lw}) * l_1 + F_{Lel} * l_2}{J} + \frac{(F_{Dfl} + F_{Dw} + F_{Del}) * l_3}{J} dtdt \tag{24}$$

2.5 Aircraft stability

2.5.1 *Static stability:*

When experiencing a disturbance, an aircraft can be statically stable, which means the reaction to the disturbance is counteracting. Further, the aircraft can be statically indifferent, which describes the behaviour of not reacting to the disturbance, or statically unstable, which means that the reaction would be indefinitely increased [18].

2.5.2 *Dynamic stability:*

To ensure the dynamic stability, the static stability is necessary, which can lead to an oscillation. Suppose the oscillation levels of the aircraft are dynamically stable. When no reaction is shown, and the oscillation remains equal it is dynamically indifferent. In the case of an increasing oscillation indefinitely, the aircraft is dynamically unstable [18].

2.5.3 *Longitudinal stability:*

When taking the neutral point of the aircraft as the reference point for the moment. The aircraft is statically stable when the centre of gravity is in front of the neutral point [19].

2.6 Frames

The movement of the aircraft and its forces can be represented in three coordinate systems. The world, body, and air frame, hence, a rotational matrix is needed.

$$R_M(\alpha) = \begin{pmatrix} cos\alpha & -sin\alpha \\ sin\alpha & cos\alpha \end{pmatrix} \tag{25}$$

The forces in the air frame can be derived as:

$$\overrightarrow{F} = \begin{pmatrix} F_D \\ F_L \end{pmatrix} \tag{26}$$

In the body frame of the aircraft, as:

$$\overrightarrow{F_b} = R_M\left(AoA_{aircraft}\right) * \begin{pmatrix} F_D \\ F_L \end{pmatrix} + \begin{pmatrix} F_e \\ 0 \end{pmatrix} \tag{27}$$

Further, a rotation in the world frame is crucial:

$$\overrightarrow{F_W} = R_M(theta) * \left(R_M\left(AoA_{aircraft}\right) * \begin{pmatrix} F_D \\ F_L \end{pmatrix} + \begin{pmatrix} F_e \\ 0 \end{pmatrix} \right) + \begin{pmatrix} 0 \\ F_G \end{pmatrix} \tag{28}$$

Due to the need of several coordinate systems, the angles of the aircraft can be defined. The angle of the speed ($v = \begin{pmatrix} \dot{X}_w \\ \dot{Z}_w \end{pmatrix}$) to the ground can be derived with the trigonometry by using: $\tan(\alpha) = \frac{\dot{Z}_w}{\dot{X}_w}$. Therefore, it is situated between the world and the air x-axis. The pitch angle (θ) can be calculated as the angle between the world frame (x_w) and the body frame (x_B). The angle of attack of the aircraft (AoA) can be calculated as the angle between the body (x_B) and the direction of the airflow (x_l). The angle of attack of the profile can be seen as the angle between the chordline and the air frame (x_l). The angle of the flaps, alpha, is situated between the chordline and the body frame (x_B).

3 Control system

3.1 Control System Configuration

The minimum components of a control system are the controller and the plant. It can be visualized with either an open-loop control system or a closed-loop control system. The main difference is that the closed-loop system has the ability to compare the desired value to the actual value, using feedback of the exact value.

A closed-loop control system is used more frequently to control complex systems and achieve precise step responses. In this system, $w(t)$ represents the desired reference for the control system target, $y(t)$ is the measured plant output, $e(t) = w(t) - y(t)$ is the error signal between the desired reference and the measured output, which serves as the controller input. $u(t)$ is the controller output that controls the plant operation, and $d(t)$ represents any disturbance to the system. It should be noted that the desired reference is often set as a flight profile for airplanes to track.

A linear system requires the following two principles to be fulfilled:

Amplification Principle:

$$v \cdot (k \cdot u) = k \cdot v \cdot (u) \tag{29}$$

Overload Principle:

$$v \cdot (u_1 + u_2) = v \cdot (u_1) + v \cdot (u_2) \tag{30}$$

In a linear system, the output size changes only when the input size changes, while a linear transfer function can approximate a nonlinear system [20]:

$$G(s) = \frac{V(s)}{U(s)} \tag{31}$$

The transfer function can be analyzed using the Laplace transformation. Following the example of a P-T_2 system , we have the differential equation:

$$\ddot{v} + 2D\omega_0\dot{v} + \omega_0^2 v = K\omega_0^2 u \tag{32}$$

The corresponding transfer function is:

$$\frac{V(s)}{U(s)} = \frac{K\omega_0^2}{s^2 + 2D\omega_0 s + \omega_0^2} \tag{33}$$

3.2 PID controller and tuning

PID controller: The most popular controller used in engineering systems is the Proportional Integral Derivative (PID) controller [21]. A typical PID controller can be functionally expressed as:

$$u(t) = K_p e(t) + \int_0^t K_i e(t)dt + K_d \frac{de(t)}{dt} \rightarrow \frac{U(s)}{E(s)} = K_p + K_{i\frac{1}{s}} + K_d s \tag{34}$$

where $e(t)$ is the controller input, normally an error between the reference $w(t)$ and the measured $y(t)$ output.

The proportional P of the controller enables the system to reach the target rapidly, but encourages overshooting. Therefore, the integral I is used to minimise the stable state error, but it can lead to an increase in the overshoot. To react proactive, the derivative D, can control the overshoot and, as a result, lead to the desired behavior.

This method applies to systems that are stabilizable by a proportional controller and enables fast, simple parameter tuning, suitable for systems pushed to their limits without causing damage. The initial K_p can be assumed or derived from step-response calculations,

and then refined using the Ziegler-Nichols tuning method.

An alternative, the Chien-Hrones-Reswick method, adjusts closed-loop parameters with a focus on permissible overshoot. Matlab's PID Tuner optimizes SISO systems by adjusting response time and robustness.

Tuning can also involve trial-and-error, PSO (for complex systems), or a structured approach: start with P, then adjust I/D values, using Ziegler-Nichols as a baseline. Values are iteratively refined based on the response, with MATLAB's tuner validating the results.

3.3 Saturation

The PID controller can be saturated to limit the output of the controller, considering the project's limitations. However, this leads to nonlinearity and can increase the model's complexity. Whereas the values in between the minimum and maximum of the saturation can be linearised. The saturation [22] can be described as:

$$u_1(t) = \begin{cases} u_{\min} \; if \; u(t) < u_{\min} \\ u_{\max} \; if \; u(t) > u_{\max} \\ u(t) \qquad\qquad else \end{cases} \tag{35}$$

4 Computational experimental demonstrations

4.1 Experimental setup

The closed control loop is divided into four components, the reference values, the controllers, the aircraft which is the plant and its calculations and the visualisation. Further, the behaviour of the aircraft can be seen in the added instruments which symbolise the cockpit of a realistic aircraft.

Regarding the flexibility and focus of the demonstration, the key point in the simulation procedure is to divide the whole demonstration process into small sessions, called sprints, to focus on ad hoc issues efficiently.

4.2 Sprint 1 - Design aircraft

The plant in the project is the aircraft model. It is simplified compared to the literature review. The wing and elevator are chosen to use the same NACA profile. Further, the aircraft dimensions are adapted to enable the centre of gravity to be situated in front of the wing to enable the stability. The forces are assumed to attack at half the length of the control surfaces, and the engine is at the same height as the centre of gravity; by choosing this, another moment can be avoided. The wing is situated in alignment with the elevator. It is visualised with a MATLAB function in Simulink.

The aircraft is modeled using a MATLAB function in Simulink, which calculates all forces and moments of an airplane in a 2D environment, as stated in the literature review. In the 2D environment, the ailerons are visualized the operating the same as flaps because of no possibility to roll along the longitudinal axis.

To calculate the lift and drag, the density is necessary. Therefore, a possible value of the density is compared to the ICAO standard atmosphere.

To implement the limitations of the NACA profile and stall characteristics, the $c_L$value is described as a maximum when the AoA reaches 12°. The $c_D$value can not exceed the maximum of the average value of a vertical plate.

As stated above, the calculation needs several coordinate systems. The forces and moment equations are calculated in the air coordinate system. Because of this, a conversion from the world coordinate system to the body coordinate system and the air coordinate system is needed to implement the external forces, such as gravity.

The world coordinate system is the system used to see the aircraft from an observer's perspective. To calculate in the body coordinate system, which is the aircraft's own coordinate system, the rotational matrix must be applied using the pitch angle.

The calculation from the body coordinate system to the air coordinate system, which demonstrates the direction of the wind's velocity, is performed using the rotational matrix and the angle of attack of the aircraft.

The angles are rotated against the y-axis, therefore the positive direction of the angles is determined by the positive direction of the y-axis and its rotation, except from the angle of the speed to the ground, which sign is determined by the calculated of the angle, while using the velocities.

After calculating the forces and moment, a back translation to the world coordinate system is performed by using the rotation matrix twice, as in the initial calculation.

To enable the calculation of the equations of motio,n the centre of gravity of the aircraft is needed, hence the surface area of the aircraft is assumed realistically,

and the centre of gravity can be calculated in the x and z direction:

$$x_s = \frac{\sum x_i * A_i}{\sum A_i} \tag{36}$$

$$z_s = \frac{\sum z_i * A_i}{\sum A_i} \tag{37}$$

The aircraft is assumed to be symmetrically, therefore the centre of gravity in the y direction is zero [**?**].

The moment of inertia (J) can be derived from:

$$J_s = \frac{m * (h^2 * b^2)}{12} \tag{38}$$

Due to the non-alignment of the centre of gravities of the different surface areas the following calculation is crucial:

$$J = J_s + r_s^2 * m \tag{39}$$

Whereas the total J is calculated by summing the previously derived values

$$J_{ges} = \sum_{n=1}^{n} J \tag{40}$$

The calculations are implemented in the Simulink model using a MATLAB function, which enables the change of aircraft type.

As seen above, the function is taking the new mass of the aircraft as an input, which is changing due to the fuel burn. The new mass can be calculated as stated below [23], where realistic values for the fuel burn are assumed:

$$m_n(t) = \int (f_b * \rho)(t)dt + C \tag{41}$$

Furthermore, the equations of motion of the system are implemented in a separate subsystem and lead back to the actual value of the state of the aircraft, which occurs to closes the loop and secures the implementation of a closed-loop system.

The aircraft is implemented successfully and can be adjusted with minor variations.

It should be noted that this aircraft model has been simplified due to the focus on the control system development.

4.3 Sprint 2 - Design PID controllers

Firstly, to control the velocity of the aircraft a PID controller is implemented which takes the desired velocity as an input and therefore controls the overall velocity. The output is shown in Figure 4.

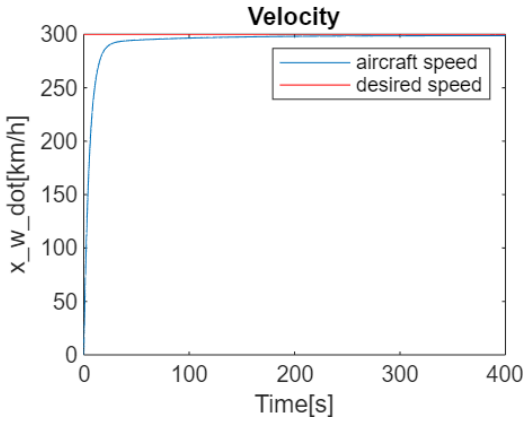

Figure 4. output engine controller.

The engine controller has the main impact on the movement along the x-axis. Which can be seen in Figure 5.

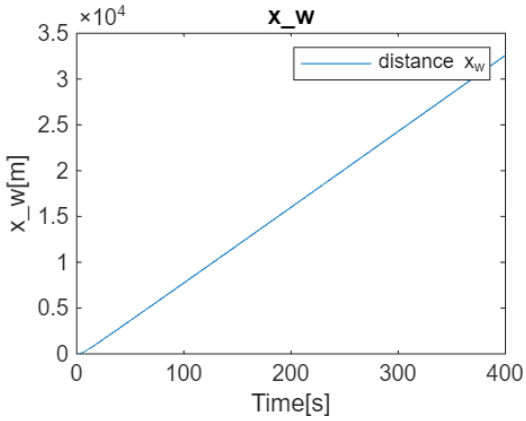

Figure 5. distance x_w.

The controller is saturated to enable a realistic acceleration of the engine from zero to 8.5 $\frac{m}{m^2}$.

Furthermore, the controller is designed to reach the desired speed quickly, without overshoot, to ensure a safe behavior of the aircraft.

Result discussion: The engine controller facilitates the aircraft to reach a desired speed quickly but without overshooting, which results in a more extended transition phase from halt to the cruise speed. However, the controller ensures a favourable behaviour.

4.4 Sprint 3 - Theta control

To create a pitch movement, a controller of the pitch angle theta is needed. Therefore, the theta controller is designed as a PID controller and can adjust to certain desired angles as shown in Figure 6.

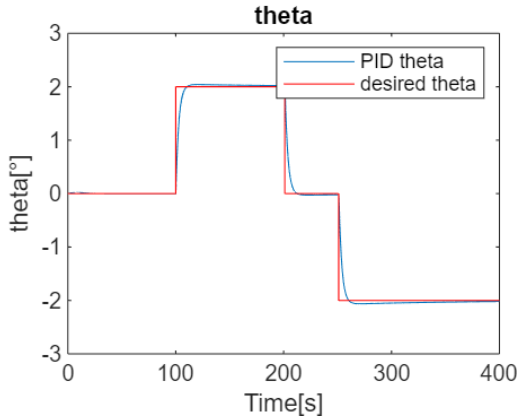

Figure 6. output theta controller.

The controller is saturated to ensure the obeying of the stall characteristics of the chosen NACA profile as stated before (literature review). Therefore, the controller is only able to operate within certain limits.

Result discussion: The theta controller is capable of maintaining the aircraft in a desired pitch angle, which can be adjusted according to a previously chosen flight profile with varying angles, resulting in a time-controlled system (literature review). Moreover, the controller rounds off the sharp edges, as seen in the desired theta, to create a realistic behavior of an aircraft and enhance passenger comfort.

4.5 Sprint 4 - Height control

The two control surfaces of the stated aircraft are the engine and the elevator. Hence the aircraft is underactuated because of three degrees of freedom in the 2D frame (x-, z-, theta movement). To overcome this issue, the height is dependent on the pitch angle, and the pitch angle itself is less important than reaching the height. Therefore, a height controller has been developed that aims to maintain the desired height as stated in the flight profile and control it in comparison with the pitch angle (see Figure 7).

The velocity in the z-direction can be measured, as shown in Figure 8. It can be used to measure the effect of the flight manoeuvres and the comfort of the passengers.

While developing the controller, it was identified that the controller works well for the higher speed chosen. While adjusting the controller's values and trying a

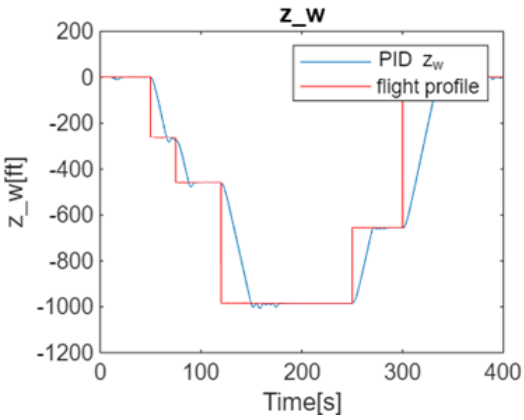

Figure 7. output z_w high speed controller.

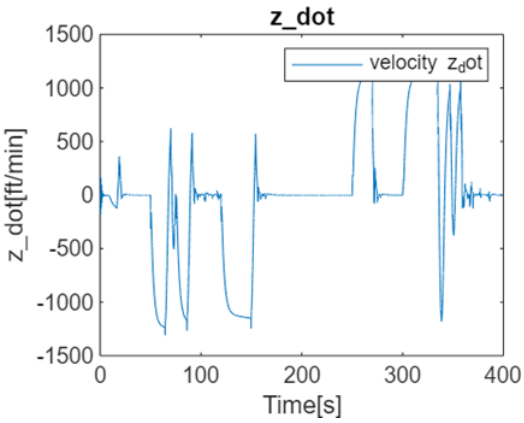

Figure 8. velocity in z-direction high speed height controller.

lower speed, a second controller was implemented (see Figure 9).

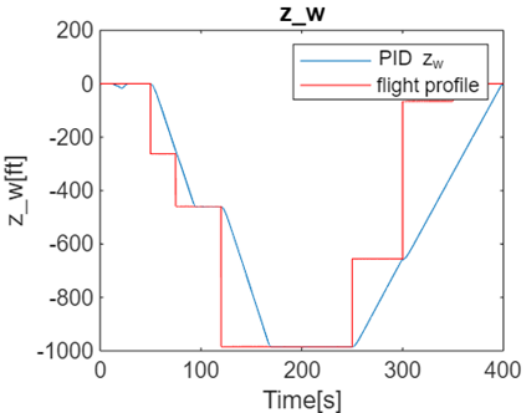

Figure 9. output z_w low speed controller.

The velocity in the z-direction is the same as for the high-speed height controller. This is shown in Figure 10.

The controllers are saturated PID controllers, chosen due to the limitations of the engine's acceleration, the stall characteristics of the profile, and the aircraft's

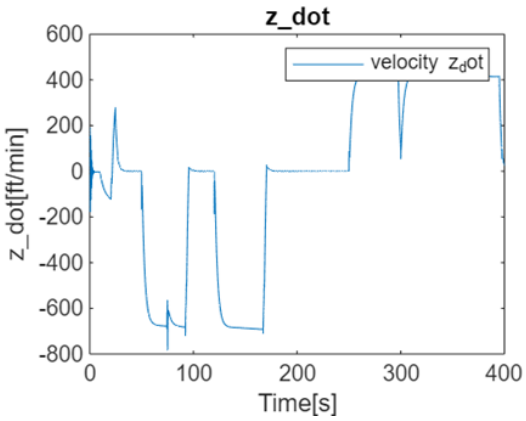

Figure 10. velocity in z-direction low speed.

situation.

However, the saturation of the height controller for lower speeds is more limited than that of the height controller for higher speeds. This is because lower speeds are often chosen at lower heights or during slow flight. Therefore, the aircraft is more affected by winds near the ground, which is why deflections of the control surfaces should be more precise.

Result discussion: Each height controller can maintain the aircraft at a scheduled height, but is limited in its operating area. Moreover, in this sprint, it was discovered that the height controller for high speed tends to overshoot the desired height while still achieving the target height within an acceptable time.

The height controller for slow speed can reach the desired height, but takes slightly more time, which is due to the avoidance of overshooting and a softer flight along the flight profile. This behavior can be observed in the velocity in the z-direction, where the high-speed height controller achieves higher speeds in an effort to reach the desired height more quickly.

However, both controllers are designed for a specific speed and can be used separately to enhance flight behavior and comfort.

4.6 Sprint 5 – Switching control of heights

Due to the acknowledges from the sprint before and the usage of two separate height controllers, a selector to differentiate between the two controllers is implemented.

Until the aircraft gains a stable velocity, the height controllers are deactivated, and a reference value below the stable speed is set. When reaching the stable velocity, a second switch either enables the low-speed or high-speed height controller, depending on the velocity.

The height controller for low speed is active below the original designed value of the height controller for high speed, due to activation at lower altitudes or during slow flight.

Result discussion: The selector enables the model to use both height controllers depending on the speed. Nonetheless, the selector slows down the simulation significantly, which can be because of the fluctuating speed while reaching the desired speed.

4.7 Limitations of the demonstrations

Due to the simplification of the aircraft model, the centre of gravity can vary from its original position in a real aircraft because of the weight of different components, such as the motor or cockpit instruments. Furthermore, the controllers developed are designed for a specific cruise speed, which results in imprecision for variable speeds.

5 Conclusion

Overall, the study enhances our understanding of both the complexities involved in fixed-wing aircraft control and the practical aspects of programming in MATLAB and integrating with Simulink, explicitly targeting the power of attitude and altitude within a 2D frame. This study has been simplified to facilitate its implementation in both analytical and simulation aspects. The chosen methodology proved effective, thanks to its iterative and adaptive nature. It has enabled the quick implementation of changes and facilitated the efficient analysis of output differences, contributing to continuous improvement throughout the development process. Specifically, simulation demonstrations have mitigated controller saturation and nonlinear dynamic effects, particularly in consideration of industrial applications. This study has provided an acceptable platform for further control system expansions with advance methods from model-based to model-free in the follow-up research and demonstrations.

Data Availability Statement

Data will be made available on request.

Funding

This work was supported without any funding.

Conflicts of Interest

The authors declare no conflicts of interest.

Ethical Approval and Consent to Participate

Not applicable.

References

[1] Raymer, D. (2012). *Aircraft design: a conceptual approach*. American Institute of Aeronautics and Astronautics, Inc.. [Crossref]

[2] Bulka, E., & Nahon, M. (2019). Automatic control for aerobatic maneuvering of agile fixed-wing UAVs. *Journal of Intelligent & Robotic Systems, 93*(1), 85-100. [Crossref]

[3] Lunze, J. (2010). *Regelungstechnik 1: Systemtheoretische grundlagen, analyse und entwurf einschleifiger regelungen*. Berlin, Heidelberg: Springer Berlin Heidelberg. [Crossref]

[4] Faradonbeh, M. K. S., Tewari, A., & Michailidis, G. (2020). On adaptive linear–quadratic regulators. *Automatica, 117*, 108982. [Crossref]

[5] Aliyu, M. D. S. (2011). *Nonlinear H∞-control, Hamiltonian systems and Hamilton-Jacobi equations*. CRC. [Crossref]

[6] Kouvaritakis, B., & Cannon, M. (2016). Model predictive control. *Switzerland: Springer International Publishing, 38*(13-56), 7. [Crossref]

[7] Mubeena, M., Mullai Venthan, S., Nisha, M. S., Senthil Kumar, P., Vijayakumar, P., & Rangasamy, G. (2025). A Survey of Autopilot Control Systems: From Classical PID to Intelligent Adaptive Controllers. *International Journal of Aeronautical and Space Sciences*, 1-26. [Crossref]

[8] Lin, F. (2007). *Robust control design: an optimal control approach*. John Wiley & Sons.

[9] Stevens, B. L., Lewis, F. L., & Johnson, E. N. (2015). *Aircraft control and simulation: dynamics, controls design, and autonomous systems*. John Wiley & Sons.

[10] Marqués, P., & Da Ronch, A. Advanced UAV Aerodynamics, Flight Stability and Control. [Crossref]

[11] Nicolai, L. M., & Carichner, G. E. (2010). *Fundamentals of aircraft and airship design: Volume I–aircraft design*. American Institute of Aeronautics and Astronautics, Inc.. [Crossref]

[12] Liu, H. H., & Zhu, B. (2018). *Formation control of multiple autonomous vehicle systems*. John Wiley & Sons. [Crossref]

[13] Anderson, J. (2023). *ISE Ebook Online Access for Fundamentals of Aerodynamics*. McGraw-Hill US Higher Ed ISE.

[14] Bohl, W., & Elmendorf, W. (1980). *Technische Strömungslehre: Stoffeigenschaften von Flüssigkeiten und Gasen, Hydrostatik, Aerostatik, inkompressible Strömungen, kompressible Strömungen, Strömungsmesstechnik*. Vogel.

[15] Ntantis, E. L., & Xezonakis, V. (2025). Aerodynamic design optimization of a NACA 0012 airfoil: An introductory adjoint discrete tool for educational purposes. *International Journal of Mechanical Engineering Education, 53*(3), 611-630. [Crossref]

[16] *Center of pressure.* (n.d.). NASA Glenn Research Center. Retrieved from https://www.grc.nasa.gov/www/k-12/VirtualAero/BottleRocket/airplane/cp.html

[17] *Extra 300 LX.* (n.d.). World of The Flying Bulls. Retrieved from https://www.flyingbulls.at/en/fleet/extra-300-lx

[18] Kassera, W. (2017). Motorflug kompakt. *Das Grundwissen zur Privatpilotenlizenz. Stuttgart*.

[19] Bender, B., & Göhlich, D. (2020). *Dubbel Taschenbuch Für Den Maschinenbau 2*. Springer Berlin/Heidelberg. [Crossref]

[20] Buchholz, J. (2016). Regelungstechnik und Flugregler. *Ergänzte Auflage*.

[21] Borase, R. P., Maghade, D. K., Sondkar, S. Y., & Pawar, S. N. (2021). A review of PID control, tuning methods and applications. *International Journal of Dynamics and Control, 9*(2), 818-827. [Crossref]

[22] Mao, Q., Xu, Y., Chen, J., Chen, J., & Georgiou, T. T. (2024). Maximization of gain/phase margins by PID control. *IEEE Transactions on Automatic Control, 70*(1), 34-49. [Crossref]

[23] Papula, L. (2009). Mathematik für Ingenieure und Naturwissenschaftler, Band 1+ 2. *Vieweg+ Teubner Verlag, Wiesbaden*. [Crossref]

Eileen Horstkötter is doing her bachelor's degree (BEng) at the University of the West of England in Bristol in cooperation with the University of applied sciences in Osnabrück, Germany from where she is receiving the BSc in aerospace engineering. (Email: e.horstkoetter@gmx.net)

Quanmin Zhu is Professor in control systems at the School of Engineering, University of the West of England, Bristol, UK. He obtained his MSc in Harbin Institute of Technology, China in 1983, PhD in Faculty of Engineering, University of Warwick, UK in 1990, and worked a as postdoctoral research associate at the Department of automatic control and systems engineering, University of Sheffield, UK between 1989-1994. His main research interest is in complex system modelling, identification, and control. He has published over 300 papers on these topics, edited various books with Springer, Elsevier, and the other publishers, and provided consultancy to various industries. Currently Professor Zhu is acting as Editor of Elsevier book series of Emerging Methodologies and Applications in Modelling, Identification and Control. (Email: quan.zhu@uwe.ac.uk)